
DOES MEDICAL SPECIALIZATION OF VLMs ENHANCE DISCRIMINATIVE POWER?: A COMPREHENSIVE INVESTIGATION THROUGH FEATURE DISTRIBUTION ANALYSIS

Keita Takeda

Graduate School of Integrated Science and Technology
Nagasaki University
ktakeda@nagasaki-u.ac.jp

Tomoya Sakai

Graduate School of Integrated Science and Technology
Nagasaki University
tsakai@nagasaki-u.ac.jp

January 22, 2026

ABSTRACT

This study investigates the feature representations produced by publicly available open source medical vision-language models (VLMs). While medical VLMs are expected to capture diagnostically relevant features, their learned representations remain underexplored, and standard evaluations like classification accuracy do not fully reveal if they acquire truly discriminative, lesion-specific features. Understanding these representations is crucial for revealing medical image structures and improving downstream tasks in medical image analysis. This study aims to investigate the feature distributions learned by medical VLMs and evaluate the impact of medical specialization. We analyze the feature distribution of multiple image modalities extracted by some representative medical VLMs across lesion classification datasets on multiple modalities. These distributions were compared them with non-medical VLMs to assess the domain-specific medical training. Our experiments showed that medical VLMs can extract discriminative features that are effective for medical classification tasks. Moreover, it was found that non-medical VLMs with recent improvement with contextual enrichment such as LLM2CLIP produce more refined feature representations. Our results imply that enhancing text encoder is more crucial than training intensively on medical images when developing medical VLMs. Notably, non-medical models are particularly vulnerable to biases introduced by overlaid text strings on images. These findings underscore the need for careful consideration on model selection according to downstream tasks besides potential risks in inference due to background biases such as textual information in images.

Keywords Vision-language models · foundation models · feature representation · CLIP · LLaVA

1 Introduction

Vision-Language Models (VLMs) are deep learning models trained on large-scale datasets to embed images and texts into their respective universal feature spaces [46]. While general VLMs have shown remarkable capabilities [46], adapting them to specialized domains is crucial. Medical image analysis, in particular, has emerged as a significant application area [47]. This field faces unique challenges, such as difficulties in acquiring large datasets due to limited cases and the critical need to analyze disease-specific image features. Consequently, as illustrated in Table. 1, numerous medical VLMs have been proposed in recent years to address these demands.

Understanding the universal features produced by these medical VLMs is paramount to assume their appropriate application to downstream tasks, especially in medical image analysis where explainability and interpretability are vital. However, research on the universal feature spaces of VLMs has often been limited to indirect evaluations, even in the natural image domain [48, 49]. Existing survey papers on medical VLMs [50, 51, 47] also tend to focus on

Table 1: Popular medical vision-language models (VLMs) and corresponding non-medical VLMs. Supported means the VLM is employed for experiment on this study. Backbone means the VLM employ the image encoder backbone. Target modality means the VLM is specialized the imaging modality.

support	model name	backbone	target modality	dataset source
Medical VLMs trained on contrastive learning manner				
✓	BiomedCLIP [1]	ViT-B/16 [2]	Modality-agnostic	Paper figure
	UniMedCLIP [3]	ViT-L/14 [2]	Modality-agnostic	Public datasets
✓	ConceptCLIP [4]	SigLIP [5]	Modality-agnostic	Paper figure
✓	MedSigLIP [6]	SigLIP [5]	Modality-agnostic	Paper figure and public datasets
	CT-CLIP [7]	CT-ViT [8] based	3D-CT	Public datasets
	Merlin [9]	3D ResNet152	3D-CT	Original
✓	CXR-CLIP [10]	SwinTransformer [11]	Chest X-ray	Public datasets
	Mammo-CLIP [12]	EfficientNet [13]	Mammography	Public datasets
✓	CONCH [14]	CoCa [15] based	Histopathology	Public datasets
	ViLa-MIL [16]	CLIP [17]	Histopathology	Public dataset
✓	UNI [3]	DINOv2 [18] (ViT-B/16 [2])	Histopathology	Original
	CHIEF [19]	CTransPath [8] based	Histopathology	Public datasets
✓	FLAIR [20]	ResNet50 [21]	Ophthalmology	Public datasets
	KeepFIT [22]	ResNet50 [21]	Ophthalmology	Books and public datasets
	VisionUite [23]	EVA02 [24] and CLIP [17] based	Ophthalmology	Public datasets
	CLIP-DR [25]	ResNet50 [21]	Ophthalmology	Public datasets
✓	MONET [26]	ViT-L/14 [2]	Dermatology	Paper figure and public datasets
	MAKE [27]	CLIP [17]	Dermatology	Paper figure and others
	DermLIP [28]	ViT-L [2]	Dermatology	Paper figure and public datasets
Medical VLMs trained on instruction tuning manner				
✓	LLaVA-Med [29]	ViT-L/14-336 [2]	Modality-agnostic	Paper figure
✓	LLaVA-Med++ [30]	ViT-L/14-336 [2]	Modality-agnostic	Paper figure and public datasets
	MedGemma [6]	MedSigLIP [6]	Modality-agnostic	Public datasets
Corresponding or popular non-medical VLMs				
✓	LLaVA [31, 32]	ViT-L/14-336 [2]	Non-medical	Public datasets
✓	EVA02 [24]	ViT-L/14-336 [2]	Non-medical	Public datasets
✓	LLM2CLIP [33]	ViT-L/14-336 [2]	Non-medical	Public datasets

evaluation via performance metrics like classification accuracy rather than re-evaluating the learned universal feature spaces. Therefore, a deeper investigation into what features are internally computed by these models and how their parameters contribute to feature extraction is essential.

To address this gap, our study analyzes the distribution of image features extracted by the image encoders of medical VLMs. We utilize eight classification datasets covering different imaging modalities. The universal image feature distributions extracted by representative medical VLMs shown in Table. 1 are visualized using dimensionality reduction.

Table 2: Specifications of datasets used for experiment

Dataset Name	Modality	task
Brain tumor classification [34] (referred to as Brain MR)	MRI	Brain tumor detection and classification
SARS-CoV-2 CTscan [35]	CT	COVID-19 diagnosis
PneumoniaMNIST [36, 37, 38]	X-ray	Diagnosis of pneumonia
Breast Ultrasound Images Dataset [39] (referred to as BreastUS)	Ultrasound	Breast tumor classification
BreakHis [40]	Histopathology	Breast tumor classification
HiCervix [41]	Cytology	Cervical cancer detection
DeepDRiD [42]	Ophthalmology	Grading retinal images for diagnosis of Diabetic retinopathy
ISIC 2019 [43, 44, 45]	Dermatology	Skin cancer detection

These are compared with feature distributions from their non-medical counterparts as well as LLM2CLIP [33] (which features an enhanced text encoder for contextual enrichment), to assess the impact of medical domain-specific training. Furthermore, since low-dimensional visualization may not fully capture a model’s ability to discern discriminative features, we construct linear discriminators to evaluate the performance of each model in its original high-dimensional feature space.

2 Motivation of developing Medical VLMs

The development of medical VLMs is driven by two primary motivations. The first is to achieve SoTA model performance. VLMs are adept at learning high-quality feature representations compared to conventional models [52, 53, 17], making it easier to outperform models trained without language labels [17]. Indeed, several medical VLMs have been evaluated to have superior performance on benchmark datasets compared to non language models such as ResNet [21] or SimCLR [54, 55]. A key byproduct of this is the facilitation of transfer learning for rare diseases [56]. Since VLMs are assumed to have learned sophisticated feature representations well-suited for a wide range of downstream tasks [1], they are expected to achieve high performance even on tasks where non VLMs struggled to overfitting [57, 56].

The second motivation is to advance medical image understanding through explanations via language. The diagnoses of medical image are still relies heavily on empirical knowledge of clinicians. While many DNN approaches have aimed to quantify and improve the empirical modeling, the subjective nature of these assessments makes them difficult to annotate, posing a challenge for traditional supervised learning. However, these empirical findings are often recorded by text in clinical reports [52]. Training VLMs with empirical descriptions as a supervision enables to quantify image features that correspond to these clinical knowledge [52]. This linkage between visual features and language also enhances model explainability.

3 Data sources for training medical VLMs

Medical VLMs requires vast amounts of data for their training. Current approaches draw from two primary data sources: aggregation of public datasets, and extraction of medical images from medical journal papers.

First, a common strategy is the aggregation of public datasets. While individual medical datasets are often too small for training large VLMs, combining them can yield a substantial volume of several million images [58, 3]. Popular portal sites include the cancer imaging archive (TCIA) [59], which hosts a comprehensive collection of cancer-related images (MRI, CT, pathology) along with clinical metadata and reports. Other valuable resources are Zenodo [60], which archives data used on experiment of research papers, and Kaggle [61], which hosts curated datasets for competitions.

While aggregating public dataset allows us to build a large dataset covered for wide-range modalities, some applications requires feature representations specialized for narrower, specific modalities. As will be discussed in Section 4, the development of modality-specific datasets is advancing to build such specialized VLMs. Constructing modality-specific datasets is typically achieved by aggregating numerous smaller datasets around a core of one or more relatively large-scale datasets, which usually contain tens of thousands of images or more.

Chest X-ray and fundus imaging are the modalities for which the construction of modality-specific datasets is particularly advanced. For chest X-ray data, two dataset, CheXpert [62] and MIMIC-CXR [63], are highly influential. CheXpert is a multi-label dataset created to assimilate the findings of radiologists. While multi-label datasets require special handling for standard classifiers, they are valuable for training foundation models as they facilitate the learning of image features that correspond to a wide range of linguistic expressions.

In the fundus imaging modality, the two most prominent datasets are EYEPACK [64] and AIROGS [65]. These are categorical datasets for the classification of diabetic retinopathy and glaucoma screening, respectively, and are substantially larger than other available datasets. A typical example of dataset aggregation in this modality is the FLAIR [57], which Rodriguez et al. constructed by integrating 38 public datasets.

For other modalities, the aggregation of public datasets is less common. A significant factor is the limited number of publicly available datasets. Particularly for MR imaging, while numerous segmentation datasets have been proposed, categorical datasets are scarce. This is due to the primary focus on detection tasks within the MR domain. Similarly, for other modalities where detection tasks are predominant, such as CT, there are fewer proposals for VLMs. Likewise, for modality such as ultrasound, where datasets are inherently scarce, the lack of data for aggregation has also limited the proposal of VLMs.

While these public datasets offer high-quality clinical images and corresponding image findings, their total volume often falls short of the tens of millions of samples used to train general-purpose VLMs. Consequently, they are typically used in conjunction with other data sources.

Another major data source is the vast repository of figures and captions within academic publications. Medical journals frequently feature clinical images, and by leveraging curated collections like PMC-OA [66] or employing large-scale web scraping [1, 67, 68, 69], researchers have been able to construct datasets in the tens of millions [1, 67, 69]. Medical papers often contain a wide range of typical and outlier cases with high-quality image captions. However, a significant drawback is the image quality itself. Publication formats are not optimized for medical imaging formats such as DICOM. High-resolution, high-bit-depth images are often compressed to meet file size constraints, which may result in the loss of important diagnostic features [70, 71, 72]. Therefore, the development of medical VLMs often relies on a hybrid approach, balancing the high-quality of public datasets with the large-quantity of data extracted from literature.

4 Popular Medical VLMs and remaining challenges

Current research in medical VLMs is primarily advancing along two main directions: modality-agnostic and modality-specific approaches. The first, modality-agnostic medical VLMs, aim to capture image features common across general medical images, without specializing in a particular domain. Table 1 shows popular VLMs and corresponding non-medical VLMs. For instance, Zhang *et al.* developed BiomedCLIP [1] by training CLIP [17] on PMC-15M, a dataset of 15 million figure-caption pairs from PubMed articles. Li *et al.* developed LLaVA-Med [29] by fine-tuning LLaVA [31] on the dataset. The performance of instruction tuned models on tasks of visual question answering (VQA) has been further improved by leveraging even larger datasets, such as MedTrinity-25M [30]. Khattak *et al.* also introduced UniMedCLIP, trained on UniMed, a 5.3 million sample dataset aggregated from public medical sources [3]. Sellergren *et al.* developed MedGemma [6] by fine-tuning Gemma on PMC-OA [66] and several public dataset. These modality-agnostic medical VLMs are expected to have a wide range of applications.

The other group, modality-specific medical VLMs, aims to learn feature extractors specialized for particular imaging modalities. By specializing in a specific imaging modality, these models enable end-to-end analysis for that modality, often with a single, tailored model. In histopathology, for example, foundation models such as CONCH [14], UNI [73], and CHIEF [19] have been developed, typically utilizing large collections of pathology images from resources like The Cancer Genome Atlas (TCGA) [74]. In ophthalmology, VisionUnite [23] has emerged as a notable model, employing a Large Language Model (LLM) as its text encoder to achieve context-aware image feature understanding based on clinical findings. Furthermore, to address the complexities of 3D medical data, Hamamci *et al.* extended the 2D CLIP architecture to 3D for learning structural features from CT volumes [7].

However, how to best leverage these foundation models remains a crucial problem. In practice, directly applying a foundation model to a wide range of tasks is uncommon. Instead, research and clinical utility are typically directed toward narrow downstream objectives, such as the fine-grained classification or localized detection of specific pathological lesions. For these specialized applications, compact and highly discriminative feature representations are frequently the most effective. By distilling necessary and sufficient feature representations from medical VLMs, which have been pre-trained on diverse datasets, researchers can develop task specific models that are both computationally efficient and robust to the domain shifts common in clinical environments.

Many existing approaches employ fine-tuning approach to build task-specific models by collecting relatively large datasets containing over a thousand images. However, it is often impossible to prepare a dataset large enough for effective fine-tuning in the medical image domain. To address these constraints, parameter-efficient fine-tuning (PEFT) and zero-shot classification have emerged as compelling alternatives. These methodologies practically assume that the VLM's latent space already encompasses a rich feature representations relevant to the downstream task. While recent benchmarks [50, 51, 47] have validated the discriminative capabilities of these approaches, often through linear probing, they primarily focus on improvements of performance metrics like accuracy or F1-score. Such evaluations may obscure whether the model is truly capturing lesion-specific semantics or merely relying on spurious correlations. Consequently, a deeper investigation into the VLM's learned universal feature space is crucial for ensuring the reliability and explainability of their outputs in diverse medical image analysis applications.

5 Discriminative capability analysis via visualization of image feature distributions

This study aims to ascertain whether medical VLMs effectively acquire discriminative features from medical specialization. To test this hypothesis, we visualizes the feature distributions extracted by representative medical VLMs across

different modalities as listed in Table 1. For comparison, we included their corresponding non-medical counterparts and other popular non-medical VLMs to assess the effectiveness of domain-specific medical training.

We investigated the modality-specific behaviour of feature extraction by observing the feature distribution of the dataset across eight modalities. We collected public datasets for MRI, CT, X-ray, ultrasound, histopathology, cytology, ophthalmology, and dermatology. These datasets are detailed in Table 2. Input images were pre-processed using the official functions provided with each VLM’s implementation.

We extended our analysis to evaluate the zero-shot transferability of modality-specific VLMs to domains outside their primary training distribution. Specifically, we applied modality specific VLMs to both closely related and functionally distinct modalities. This assessment is predicated on the hypothesis that VLMs trained on large-scale datasets of distinct modalities may develop superior feature representations that surpass those of models trained on smaller, domain-relevant datasets. By including seemingly unrelated modalities, we aim to verify the extent to which data scale and inherent feature complexity influence cross-modal representation learning.

To qualitatively assess the discriminative ability of the extracted image features, we reduced them to two dimensions using UMAP [75] and visualized the resulting distributions. We employed the Python implementation provided by Sainburg *et al.* [76]. As most VLMs are trained via contrastive learning to enhance cosine similarity, we selected the `cosine` metric for UMAP optimization. While we conducted an extensive grid search over the `n_neighbors` and `min_dist` hyperparameters and analyzed the resulting distributions across all configurations, we present only the most representative visualizations that effectively characterize the observed feature properties.

Furthermore, since visualization of reduced-dimensional features alone may not fully reflect the ability of VLMs to capture discriminative features, we constructed a linear discriminator to evaluate the performance in the original high-dimensional feature space. For training the image classifiers, 20% of the data (from the official training set, or the combined training and validation set where applicable) was held out as the test set. The remaining data were used for training with five-fold cross-validation.

We employed a linear SVM from `scikit-learn` [77] implementation as the discriminator. All feature vectors were standardized before training. The SVM hyperparameter C was set as $C = t d_e / N$, where the optimal t was determined via grid search. Here, d_e denotes the number of dimension of the feature vector extracted by each model, and N is the number of training samples. The parameter t was selected from $\{1, 10, 100, 1000, 10000\}$ to maximize the F1-score on the validation data. These parameters were sufficient to saturate the F1-score on the training and validation data; fundamentally, the classification performance on the validation data remained roughly equivalent regardless of which of these hyperparameters was utilized.

Finally, to qualitatively assess which image regions contributed to the classification, a qualitative evaluation of model attention was conducted. After training the linear classifier, the attention maps were visualized using RISE [78] for the complete classification pipeline (i.e., the VLM encoder followed by the trained linear SVM). The number of random mask generations, N , was set to 4096.

5.1 The VLMs can be expected to classify tumors

The VLMs demonstrate the ability to acquire discriminative features related to the presence and malignancy of lesions. Figure 1(a) shows the feature distribution for the brain MR tumor classification dataset via LLM2CLIP [33]. Four distinct clusters are formed: three corresponding to the different anatomical planes, and a fourth primarily composed of images without tumors. Within these clusters, data points are discriminatively distributed regarding tumor type.

Furthermore, we constructed a linear discriminator and visualized its attention using RISE [78]. The resulting attention maps, shown in Figure 1(b). A discriminator pay attention on the tumor regions for classification. This indicates that the VLMs successfully learned discriminative features for both the presence and malignancy of tumors.

These findings were consistent across nearly all datasets and VLMs evaluated, including the non-medical VLMs. Consequently, for the datasets examined in this study, we did not observe a significant advantage from specializing the models on medical images.

5.2 Medical VLMs are affected by background biases

The feature distributions produced by the VLMs are strongly influenced by background biases present in the images. Figure 2 shows the feature distributions on Breast US dataset, and illustrates the effect of background biases. Breast US dataset contains images with overlaid textual notes and graphical annotations. ALL VLMs form distinct clusters based on these non-diagnostic, background elements. Notably, the models extract features discriminative for the semantic meaning of the overlaid words. The two small clusters at the bottom of Figure 2 are segmented based on the meaning

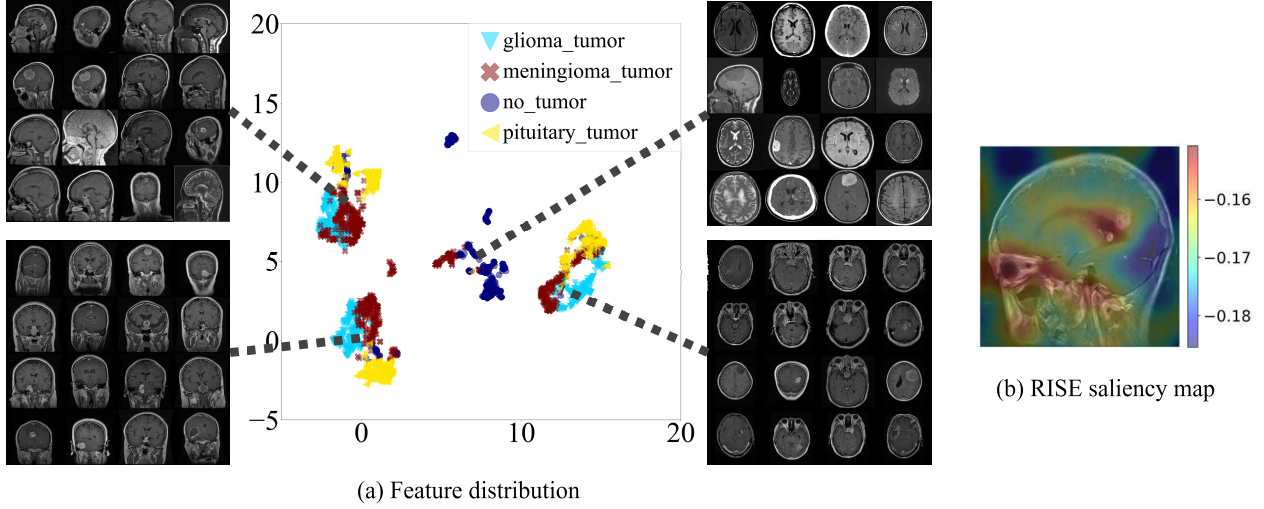


Figure 1: A example of feature distribution on Brain MR [34] dataset and corresponding RISE saliency maps. (a) Feature distribution and example images from the Brain MR [34], generated via LLM2CLIP [33]. Three clusters are formed according to the anatomical plane, with the central cluster primarily composed of images without tumors. (b) A class activation map from the LLM2CLIP and linear SVM classifiers. The model focus on the lesion area and the orbital region.

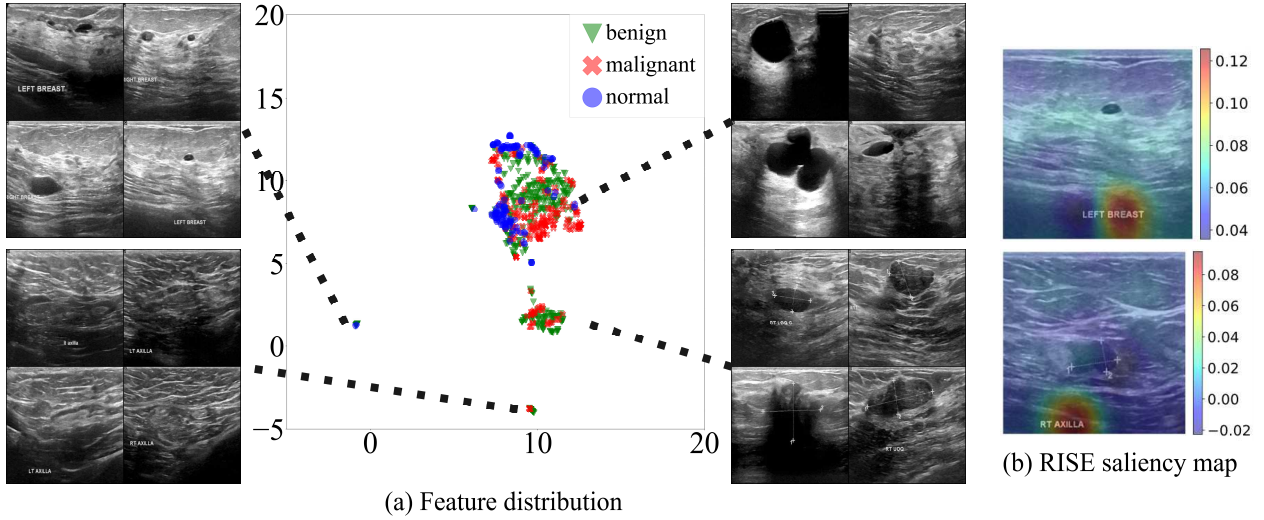


Figure 2: A example of feature distribution on the breast US [39] Dataset and corresponding RISE saliency maps. (a) Feature distribution and example images from the Breast Ultrasound Images Dataset [39], generated via LLaVA-Med. The upper-left and lower-left images are labeled as 'BREAST' and 'AXILLA,' respectively. The tumours in the lower-right images are annotated with lines. (b) Class activation map from the LLM2CLIP and linear SVM classifiers. The model focus on the textual bias written on images.

of the text, with clusters forming around anatomical terms like "Breast" and "Axilla" rather than simple directional words like "Left" or "Right". This background text effects are already reported as [79] in natural image domain. The VLMs formed another cluster based on the presence of line annotations. This sensitivity to background biases are observed across all datasets where such elements are present.

To confirm that these biases are being used for classification, we visualized the attention of a linear classifier using RISE, as shown in Figure 2(b). The attention maps clearly show that the classifier focuses on the words "Breast" and "Axilla," confirming that background information are leveraged for discrimination. While this demonstrates the VLM's capability to capture a wide range of visual information, it also highlights a significant risk: if not properly

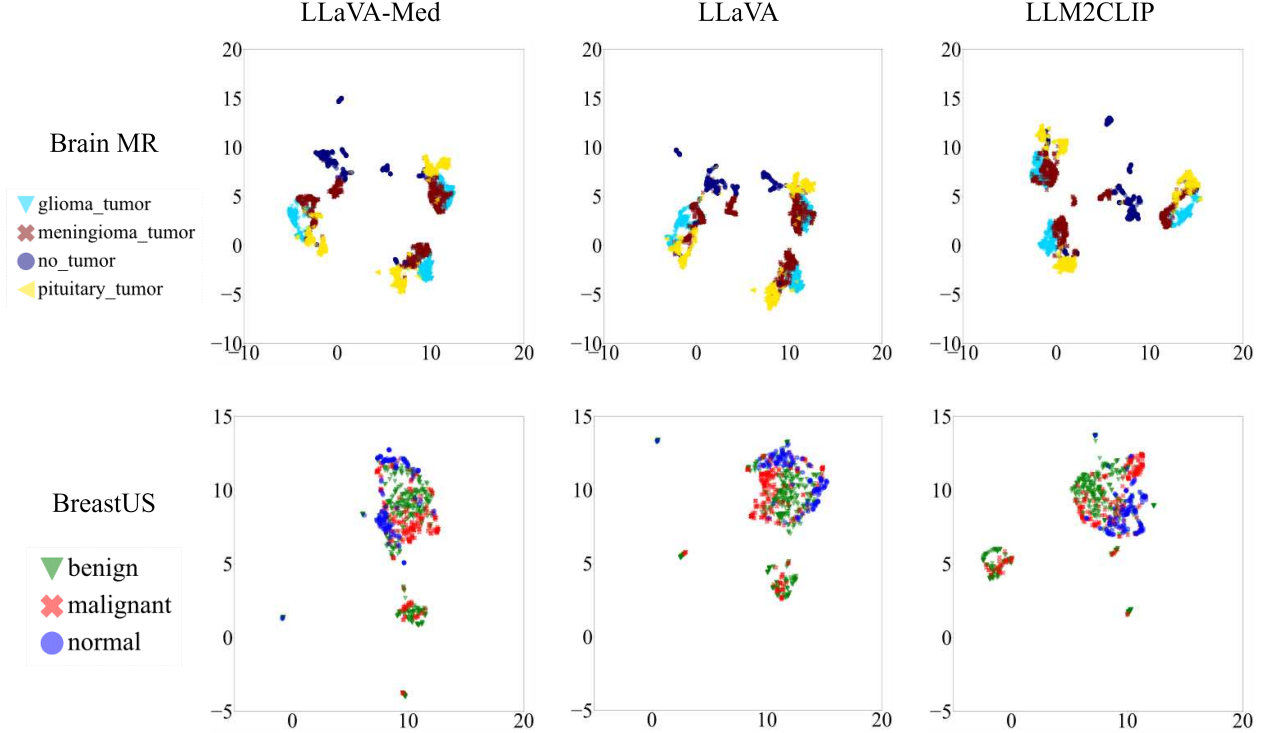


Figure 3: Examples of feature distributions for LLaVA-Med, its non-medical counterpart LLaVA, and LLM2CLIP employing an LLM as its text encoder. The upper row shows distributions in Brain MR [34], while the lower row shows distributions in Breast US [39]. No significant differences are observed in the feature distributions between LLaVA-Med and other non-medical VLMs employing an LLM as their text encoder.

addressed, models may rely on these spurious correlations during inference. Importantly, no significant difference about the effect of background bias are observed between medical-specialized and non-medical VLMs.

5.3 Medical specialization doesn't specialize image encoders

In our experiments, a qualitative analysis of the feature distributions did not reveal a clear advantage for models specialized in medical images. Figure 3 shows examples of feature distribution via medical and corresponding non-medical VLMs. For instance, the distribution from LLaVA-Med shows no significant qualitative difference when compared to others from its non-medical counterparts. This suggests that, at least in terms of the visualized feature space structure, specialization on medical data alone does not guarantee a more organized or discriminative representation.

The quantitative evaluation, presented in Tables 3 and 4, provides further insights into the discriminative capabilities of the high-dimensional feature spaces. Models employing an LLM as their text encoder, such as LLM2CLIP and LLaVA, achieved remarkable classification scores despite lacking pre-training on medical data. Notably, on the ISIC 2019 dataset, LLM2CLIP outperformed MONET, a dermatology-specific VLM. Furthermore, LLM2CLIP demonstrated accuracy comparable to FLAIR, a VLM explicitly pre-trained on the DeepDRiD dataset. In the pathology domain, UNI, a foundation model trained in a self-supervised manner on one billion image patches, surpassed nearly all other models. These results suggest that enhancing the text encoder with an LLM may be more impactful for feature discrimination than simply amassing tens of millions of medical images for pre-training.

The strong performance of LLM2CLIP and other VLMs employing LLM can be attributed to its enhanced text encoder, which implies that previous models may not have fully leveraged the rich information contained in textual descriptions. Indeed, models incorporating LLMs, such as LLaVA and LLaVA-Med, consistently achieve high scores. Moreover, MedSigLIP, a modality-agnostic model that also uses an LLM, demonstrates even better performance. Therefore, a crucial direction for improving image feature extraction in medical VLMs is to enhance the text encoder, followed by re-training on medical data to fine-tune the representations.

Table 3: Classification test accuracy and macro F1-score for models across datasets. "†" indicates the modality is included in training set. "*" indicates the dataset is included in training dataset of the model.

model name	Brain MR [34] <i>n</i> = 2,870		SARS-COV-2 CTscan [35] <i>n</i> = 2,481		PneumoniaMNIST [36, 37, 38] <i>n</i> = 4,708		BreastUS [39] <i>n</i> = 780	
	2 classes	Accuracy	2 classes	Accuracy	F1-score	Accuracy	3 classes	F1-score
Medical VLMs								
MedSigLIP	97 ± 0.5%†	97 ± 0.5%†	95 ± 0.2%†	95 ± 0.2%†	98 ± 0.3%†	97 ± 0.3%†	82 ± 2.3%†	79 ± 2.3%†
BiomedCLIP [1]	91 ± 0.5%†	91 ± 0.5%†	92 ± 0.6%†	92 ± 0.6%†	97 ± 0.1%†	96 ± 0.1%†	74 ± 2.0%†	71 ± 2.0%†
ConceptCLIP [30]	95 ± 0.7%†	95 ± 0.7%†	94 ± 0.5%†	94 ± 0.5%†	97 ± 0.3%†	96 ± 0.3%†	78 ± 1.5%†	77 ± 1.5%†
LLaVA-Med [29]	93 ± 0.2%†	93 ± 0.2%†	95 ± 0.4%†	95 ± 0.4%†	96 ± 0.2%†	95 ± 0.2%†	82 ± 1.5%†	80 ± 1.5%†
LLaVA-Med++ [30]	93 ± 0.5%†	93 ± 0.5%†	94 ± 0.1%†	94 ± 0.1%†	96 ± 0.5%†	95 ± 0.5%†	80 ± 1.4%†	78 ± 1.4%†
Modality-specific VLMs or large-scale medical pre-trained foundation models								
CXR-CLIP [10]	85 ± 0.7%	85 ± 0.7%	76 ± 1.5%	76 ± 1.5%	92 ± 0.5%†	90 ± 0.5%†	70 ± 1.9%	65 ± 1.9%
CONCH [14]	91 ± 1.1%	91 ± 1.1%	92 ± 0.3%	92 ± 0.3%	97 ± 0.2%	96 ± 0.2%	79 ± 1.4%	75 ± 1.4%
UNI [73]	93 ± 0.3%	93 ± 0.3%	96 ± 0.1%	96 ± 0.1%	97 ± 0.2%	97 ± 0.2%	77 ± 2.7%	74 ± 2.7%
FLAIR [57]	88 ± 0.4%	88 ± 0.4%	91 ± 0.7%	91 ± 0.7%	95 ± 0.3%	94 ± 0.3%	73 ± 1.5%	67 ± 1.5%
MONET [57]	92 ± 0.4%	92 ± 0.4%	94 ± 0.5%	94 ± 0.5%	96 ± 0.4%	95 ± 0.4%	77 ± 2.1%	73 ± 2.1%
non-medical VLMs								
CLIP (B/16) [17]	91 ± 0.2%	91 ± 0.2%	90 ± 0.8%	90 ± 0.8%	96 ± 0.4%	95 ± 0.4%	78 ± 2.3%	75 ± 2.3%
CLIP (L/14) [17]	90 ± 0.9%	90 ± 0.9%	89 ± 0.6%	89 ± 0.6%	96 ± 0.4%	95 ± 0.4%	77 ± 1.0%	74 ± 1.0%
CLIP (G/14) [17]	89 ± 0.8%	89 ± 0.8%	92 ± 0.5%	92 ± 0.5%	97 ± 0.4%	96 ± 0.4%	81 ± 1.9%	79 ± 1.9%
EVA02 [24]	93 ± 0.4%	93 ± 0.4%	93 ± 0.5%	93 ± 0.5%	98 ± 0.4%	97 ± 0.4%	78 ± 1.4%	74 ± 1.4%
SigLIP [30]	95 ± 0.7%	95 ± 0.7%	90 ± 0.6%	90 ± 0.6%	95 ± 0.4%	94 ± 0.4%	78 ± 1.8%	75 ± 1.8%
LLaVA [31, 32]	92 ± 0.5%	92 ± 0.5%	93 ± 0.4%	93 ± 0.4%	96 ± 0.1%	95 ± 0.1%	78 ± 1.1%	75 ± 1.1%
LLM2CLIP [33]	94 ± 0.6%	94 ± 0.6%	93 ± 0.4%	93 ± 0.4%	97 ± 0.4%	96 ± 0.4%	82 ± 0.9%	79 ± 0.9%
non VLMs								
VGG16 [80]	81 ± 0.6%	81 ± 0.6%	90 ± 0.7%	90 ± 0.7%	94 ± 0.3%	92 ± 0.3%	73 ± 1.3%	69 ± 1.3%
ResNet50 [21]	88 ± 1.0%	88 ± 1.0%	94 ± 0.3%	94 ± 0.3%	97 ± 0.3%	96 ± 0.3%	73 ± 2.0%	69 ± 2.0%
ViT-L-16 [2]	92 ± 0.6%	92 ± 0.6%	90 ± 0.6%	90 ± 0.6%	96 ± 0.5%	95 ± 0.5%	73 ± 2.1%	69 ± 2.1%
DINOv2	92 ± 0.5%	92 ± 0.5%	94 ± 0.6%	94 ± 0.6%	97 ± 0.4%	96 ± 0.4%	76 ± 0.6%	73 ± 0.6%

5.4 Negative effect of pre-training on PMC-15M

While our analysis of feature distributions did not consistently show an advantage for medical-specialized models, we identified instances where such specialization led to inferior feature extraction. Figure 3 illustrates this by visualizing the feature distributions for microbe subclasses in cervical cytology images. Compared to the three distributions on the left, those on the right exhibit a more discriminative structure, forming distinct clusters for each class. The models on the left are modality-agnostic VLMs primarily trained on the PMC-15M dataset, which is sourced from medical papers and likely contains some cervical cytology images. In contrast, the models on the right, a non-medical VLM (top) and a modality-specific model trained on a different modality (bottom), are not specialized on cervical cytology images. This leads to the counter-intuitive finding that features from models trained for general medical use can be less discriminative than those from non-medical VLMs for this task.

We attribute this nature to the quality of the publication-derived data. As reported by Zhang *et al.*, PMC-15M contains a significant number of non-medical images, such as statistical figures, flowcharts, and mathematical formulas. While training on such noisy data may enable a model to distinguish between medical and non-medical images, it can degrade its ability to extract fine-grained features from high-quality, clean data. The cervical cytology images used in this study are of high quality, lacking background biases like overlaid text. For such data, non-medical VLMs trained on massive, curated datasets or modality-specific models trained on high-quality data may extract more discriminative features. Although cervical cytology is a crucial task, it is not as common as major modalities like MRI or pathology. Consequently, for less common tasks involving high-quality images, leveraging a modality-agnostic medical VLM is not necessarily the optimal choice. As our results in Section 5.3 suggest, models that employ an LLM as the text encoder may represent a better alternative.

Table 4: Classification test scores for the other modalities than Table 3.

model name	BreakHis [40]		HiCervix [41]		DeepDRiD [42]		ISIC 2019 [43, 44, 45]	
	$n = 7,909$	2 classes	$n = 28,160$	29 classes	$n = 1,200$	5 classes	$n = 25,331$	9 classes
	Accuracy	F1-score	Accuracy	F1-score	Accuracy	F1-score	Accuracy	F1-score
Medical VLMs								
MedSigLIP	87 ± 1.4% [†]	90 ± 1.4% [†]	64 ± 0.2%[†]	60 ± 0.2%[†]	66 ± 2.0% [†]	56 ± 2.0% [†]	77 ± 0.2%[†]	65 ± 0.2%[†]
BiomedCLIP [1]	86 ± 0.9% [†]	89 ± 0.9% [†]	58 ± 0.3% [†]	54 ± 0.3% [†]	55 ± 1.1% [†]	42 ± 1.1% [†]	71 ± 0.1% [†]	54 ± 0.1% [†]
ConceptCLIP [30]	86 ± 0.4% [†]	89 ± 0.4% [†]	61 ± 0.1% [†]	58 ± 0.1% [†]	55 ± 1.6% [†]	42 ± 1.6% [†]	75 ± 0.3% [†]	61 ± 0.3% [†]
LLaVA-Med [29]	86 ± 0.9% [†]	89 ± 0.9% [†]	54 ± 0.4% [†]	51 ± 0.4% [†]	57 ± 1.5% [†]	48 ± 1.5% [†]	73 ± 0.2% [†]	58 ± 0.2% [†]
LLaVA-Med++ [30]	85 ± 1.3% [†]	88 ± 1.3% [†]	54 ± 0.5% [†]	52 ± 0.5% [†]	57 ± 1.0% [†]	47 ± 1.0% [†]	73 ± 0.4% [†]	57 ± 0.4% [†]
Modality-specific VLMs or large-scale medical pre-trained foundation models								
CXR-CLIP [10]	81 ± 0.6%	86 ± 0.6%	46 ± 0.4%	41 ± 0.4%	50 ± 2.4%	35 ± 2.4%	61 ± 0.3%	33 ± 0.3%
CONCH [14]	89 ± 0.6% [†]	91 ± 0.6% [†]	59 ± 0.4%	55 ± 0.4%	55 ± 3.0%	45 ± 3.0%	72 ± 0.2%	55 ± 0.2%
UNI [73]	91 ± 0.9%[†]	93 ± 0.9%[†]	62 ± 0.3%	59 ± 0.3%	57 ± 1.6%	46 ± 1.6%	74 ± 0.2%	61 ± 0.2%
FLAIR [57]	83 ± 1.1%	88 ± 1.1%	53 ± 0.3%	48 ± 0.3%	67 ± 2.0%*	61 ± 2.0%*	66 ± 0.3%	44 ± 0.3%
MONET [57]	85 ± 1.3%	88 ± 1.3%	59 ± 0.3%	55 ± 0.3%	52 ± 2.7%	41 ± 2.7%	74 ± 0.1% [†]	59 ± 0.1% [†]
non-medical VLMs								
CLIP (B/16) [17]	84 ± 1.0%	87 ± 1.0%	57 ± 0.1%	54 ± 0.1%	51 ± 2.6%	41 ± 2.6%	71 ± 0.3%	51 ± 0.3%
CLIP (L/14) [17]	84 ± 1.2%	87 ± 1.2%	58 ± 0.3%	54 ± 0.3%	50 ± 3.0%	39 ± 3.0%	73 ± 0.1%	56 ± 0.1%
CLIP (G/14) [17]	84 ± 0.7%	88 ± 0.7%	58 ± 0.2%	54 ± 0.2%	55 ± 1.8%	42 ± 1.8%	74 ± 0.3%	60 ± 0.3%
EVA02 [24]	85 ± 0.4%	88 ± 0.4%	60 ± 0.2%	56 ± 0.2%	52 ± 2.3%	39 ± 2.3%	75 ± 0.2%	61 ± 0.2%
SigLIP [30]	85 ± 1.2%	88 ± 1.2%	59 ± 0.4%	56 ± 0.4%	53 ± 1.3%	42 ± 1.3%	76 ± 0.2%	61 ± 0.2%
LLaVA [31, 32]	86 ± 1.0%	89 ± 1.0%	56 ± 0.5%	53 ± 0.5%	57 ± 2.2%	49 ± 2.2%	74 ± 0.3%	61 ± 0.3%
LLM2CLIP [33]	87 ± 0.7%	90 ± 0.7%	60 ± 0.4%	57 ± 0.4%	59 ± 1.4%	47 ± 1.4%	76 ± 0.3%	64 ± 0.3%
non VLMs								
VGG16 [80]	82 ± 0.6%	86 ± 0.6%	51 ± 0.2%	47 ± 0.2%	50 ± 0.6%	37 ± 0.6%	65 ± 0.2%	40 ± 0.2%
ResNet50 [21]	85 ± 0.9%	88 ± 0.9%	50 ± 0.3%	46 ± 0.3%	51 ± 0.9%	37 ± 0.9%	68 ± 0.2%	50 ± 0.2%
ViT-L-16 [2]	85 ± 1.5%	88 ± 1.5%	58 ± 0.4%	54 ± 0.4%	53 ± 1.2%	42 ± 1.2%	73 ± 0.4%	59 ± 0.4%
DINOv2	85 ± 0.9%	88 ± 0.9%	58 ± 0.2%	54 ± 0.2%	59 ± 2.5%	51 ± 2.5%	77 ± 0.1%	65 ± 0.1%

6 Limitations

While this paper has demonstrated the capabilities and weaknesses of existing medical VLMs, their superiority is assumed to vary for tasks beyond two-dimensional image classification. For instance, our investigation has not extended to tasks involving the analysis of 3D volume data, the utilisation of WSI on pathology, or multi-modal image analysis. As some VLMs for volume data [7] and WSI analysis [73] have been emerged, these models would clearly hold an advantage over existing models.

This study focuses exclusively on the analysis of image-level features. However, the primary contribution of VLMs lies in the integration of visual and linguistic representations within a embedding space. Modality-specific models, in particular, are expected to learn domain-specific linguistic patterns and clinical terminologies that frequently occur within their respective fields. Such specialization likely enhances performance in zero-shot classification tasks by leveraging the capabilities of the text encoder. While the present work provides insights into visual feature distributions, a comprehensive investigation into text-based features and their alignment with images remains a critical direction for future research. Further exploration of how textual cues influence the formation of the universal feature space will be essential to fully elucidating the potential of medical VLMs.

Local image representations are also out of scope of this study. In medical image processing, there is often significant interest in feature representations within local regions of interest, such as tumour areas. Indeed, numerous medical segmentation foundation models have been derived to meet this demand. By verifying local feature representations, we can expect to uncover new insights, such as eliminating the significant background bias demonstrated in this research and elucidating the relationship between anatomical structures and tumour features.

In this paper, there are a number of VLMs that were mentioned in Table. 1, but it is noted that some of these could not be experimented with. The primarily reason of this is the difficulties of preparing experimental environment. To illustrate this point, consider the example of LLaVA: with the advent of LLaVA-NeXT [81], a new class for

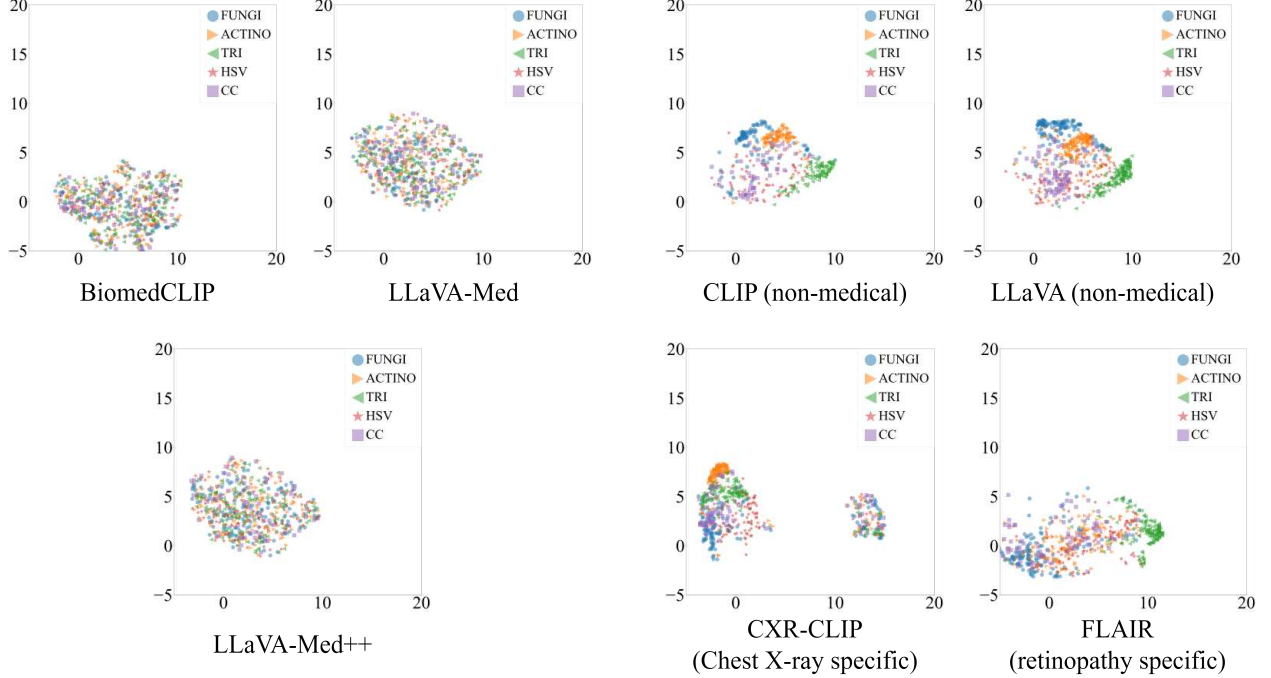


Figure 4: Feature distributions in microbe subclasses on HiCervix [41] by LLMs trained on PMC-15M [1] and other VLMs. The three on the left (BiomedCLIP [1], LLaVA-Med [29], LLaVA-Med++ [30]) are feature distributions from modality-agnostic VLMs trained on PMC-15M, which can be assumed to include cytological images. The two on the upper right (CLIP [17], LLaVA [31, 32]) are non-medical VLMs. The CXR-CLIP [10] and FLAIR [20] on the lower right are VLMs specialised for modalities other than cytology, and cytological images were not included in their training data. The model trained on PMC-15M shows no disentangled cluster within the subclasses. Conversely, the VLM on the right, which did not learn cervical images, exhibits a clear cluster structure for each subclass.

LLaVA was defined. LLaVA for natural images could be loaded with warnings now, but llava-med, which is stored in Hugging Face, generates errors when loaded and are unavailable (confirmed in version 4.57.1). This issue was traced back to a deficiency in the config file.

Another limitation of this study is about preprocessing of medical images. In our experiments, we utilized the default pre-processing functions provided with each official implementation of VLM. These functions are typically optimized for standard 8-bit RGB color images (e.g., PNG or JPEG formats). However, in clinical practice, medical images are often consists in DICOM format and consists of grayscale images with a high dynamic range (e.g., 12-bit or 16-bit depth), which differs significantly from the distributions of natural images. While specialized pre-processing is essential to handle the unique value ranges and bit depths of medical modalities, the robustness of existing VLMs to these diverse data formats remains largely unverified. Since feature extraction is highly sensitive to initial transformations such as normalization and bit-depth rescaling, the choice of pre-processing likely exerts a substantial influence on the resulting latent representations. Consequently, identifying the optimal pre-processing strategies to maximize the performance of medical VLMs for specific downstream tasks remains an important direction for future research.

This predicament carries significant ramifications, including the protracted development of medical VLMs, even within substantial teams, and the uncertainty surrounding their sustained utilisation. In particular, the transformers [82], that is to say the Hugging Face readout library and the main repository for many VLMs, is frequently specified and modified to suit the latest models. This has resulted in considerable challenges in terms of reading out medical VLMs through conventional means. This is primarily due to the fact that specification changes are primarily focused on the latest non-medical VLMs, which often results in medical VLMs being unable to adapt to these new specifications and being unable to be read out. Of course, it is possible to make them work by adjusting the library version, but this requires a lot of effort. The preparation of a distinct environment for each comparison is expensive, even if a virtual environment such as Docker is used, and it can be difficult to unify the experimental environment due to differences in library versions. Such difficulties in building a development environment are considered to be one of the reasons for the slow development of medical VLM.

7 Conclusion

This study investigated the feature distributions of medical and non-medical VLMs to assess the true impact of medical specialization. Our analysis across eight diverse medical imaging datasets revealed a key insight: the benefits of specializing a VLM’s image encoder on medical data are not as clear-cut as expected.

A principal finding is that enhancing text encoder is often more crucial than the image encoder’s medical pre-training. We found that non-medical VLMs with enhanced text encoders produced highly refined features. Consequently, their classification performance was competitive with, and sometimes superior to, specialized medical models.

Furthermore, our experiments uncovered a significant vulnerability in both medical and non-medical VLMs: a strong susceptibility to background bias. We found that models are easily fooled by spurious information, such as overlaid text annotations. Attention maps confirmed that classifiers often rely on this non-diagnostic data, posing a significant risk for clinical deployment.

We also observed a counter-intuitive result: some medical VLMs produced less discriminative features than non-medical models when analyzing clean images. This was especially true for models trained on large, noisy, publication-derived datasets like PMC-15M. This suggests that poor-quality pre-training data can degrade a model’s ability to extract fine-grained features.

These findings suggest a strategic shift for developing medical VLMs. Future efforts may benefit more from enhancing the text encoder’s contextual understanding (e.g., using LLMs) rather than pre-training image encoders on massive, noisy datasets. A more effective approach may be to combine a strong text encoder with fine-tuning on high-quality, curated medical data. Future work should extend this analysis to text features, tasks beyond 2D classification (like 3D or WSI analysis), and local feature representations.

References

- [1] Sheng Zhang, Yanbo Xu, Naoto Usuyama, Hanwen Xu, Jaspreet Bagga, Robert Tinn, Sam Preston, Rajesh Rao, Mu Wei, Naveen Valluri, et al. Biomedclip: a multimodal biomedical foundation model pretrained from fifteen million scientific image-text pairs. *arXiv preprint arXiv:2303.00915*, 2023.
- [2] Alexey Dosovitskiy, Lucas Beyer, Alexander Kolesnikov, Dirk Weissenborn, Xiaohua Zhai, Thomas Unterthiner, Mostafa Dehghani, Matthias Minderer, Georg Heigold, Sylvain Gelly, Jakob Uszkoreit, and Neil Houlsby. An image is worth 16x16 words: Transformers for image recognition at scale. In *International Conference on Learning Representations*, 2021.
- [3] Muhammad Uzair Khattak, Shahina Kunhimon, Muzammal Naseer, Salman Khan, and Fahad Shahbaz Khan. Unimed-clip: Towards a unified image-text pretraining paradigm for diverse medical imaging modalities. *arXiv preprint arXiv:2412.10372*, 2024.
- [4] Yuxiang Nie, Sunan He, Yequan Bie, Yihui Wang, Zhixuan Chen, Shu Yang, Zhiyuan Cai, Hongmei Wang, Xi Wang, Luyang Luo, et al. An explainable biomedical foundation model via large-scale concept-enhanced vision-language pre-training. *arXiv preprint arXiv:2501.15579*, 2025.
- [5] Xiaohua Zhai, Basil Mustafa, Alexander Kolesnikov, and Lucas Beyer. Sigmoid loss for language image pre-training. In *Proceedings of the IEEE/CVF International Conference on Computer Vision (ICCV)*, pages 11975–11986, October 2023.
- [6] Andrew Sellergren, Sahar Kazemzadeh, Tiam Jaroensri, Atilla Kiraly, Madeleine Traverse, Timo Kohlberger, Shawn Xu, Fayaz Jamil, Cian Hughes, Charles Lau, et al. Medgemma technical report. *arXiv preprint arXiv:2507.05201*, 2025.
- [7] Ibrahim Ethem Hamamci, Sezgin Er, Furkan Almas, Ayse Gulnihan Simsek, Seval Nil Esirgun, Irem Dogan, Muhammed Furkan Dasdelen, Omer Faruk Durugol, Bastian Wittmann, Tamaz Amiranashvili, Enis Simsar, Mehmet Simsar, Emine Bensu Erdemir, Abdullah Alanbay, Anjany Sekuboyina, Berkan Lafci, Christian Blauthgen, Mehmet Kemal Ozdemir, and Bjoern Menze. Developing generalist foundation models from a multimodal dataset for 3d computed tomography, 2024.
- [8] Xiyue Wang, Sen Yang, Jun Zhang, Minghui Wang, Jing Zhang, Wei Yang, Junzhou Huang, and Xiao Han. Transformer-based unsupervised contrastive learning for histopathological image classification. *Medical image analysis*, 81:102559, 2022.
- [9] Louis Blankemeier, Joseph Paul Cohen, Ashwin Kumar, Dave Van Veen, Syed Jamal Safdar Gardezi, Magdalini Paschali, Zhihong Chen, Jean-Benoit Delbrouck, Eduardo Reis, Cesar Truyts, et al. Merlin: A vision language foundation model for 3d computed tomography. *Research Square*, pages rs–3, 2024.

[10] Kihyun You, Jawook Gu, Jiyeon Ham, Beomhee Park, Jiho Kim, Eun K Hong, Woonhyuk Baek, and Byungseok Roh. Cxr-clip: Toward large scale chest x-ray language-image pre-training. In *International Conference on Medical Image Computing and Computer-Assisted Intervention*, pages 101–111. Springer, 2023.

[11] Ze Liu, Yutong Lin, Yue Cao, Han Hu, Yixuan Wei, Zheng Zhang, Stephen Lin, and Baining Guo. Swin transformer: Hierarchical vision transformer using shifted windows. In *Proceedings of the IEEE/CVF International Conference on Computer Vision (ICCV)*, pages 10012–10022, October 2021.

[12] Shantanu Ghosh, Clare B Poynton, Shyam Visweswaran, and Kayhan Batmanghelich. Mammo-clip: A vision language foundation model to enhance data efficiency and robustness in mammography. In *International conference on medical image computing and computer-assisted intervention*, pages 632–642. Springer, 2024.

[13] Mingxing Tan and Quoc Le. Efficientnet: Rethinking model scaling for convolutional neural networks. In *International conference on machine learning*, pages 6105–6114. PMLR, 2019.

[14] Ming Y Lu, Bowen Chen, Drew FK Williamson, Richard J Chen, Ivy Liang, Tong Ding, Guillaume Jaume, Igor Odintsov, Long Phi Le, Georg Gerber, et al. A visual-language foundation model for computational pathology. *Nature Medicine*, 30:863–874, 2024.

[15] Jiahui Yu, Zirui Wang, Vijay Vasudevan, Legg Yeung, Mojtaba Seyedhosseini, and Yonghui Wu. Coca: Contrastive captioners are image-text foundation models, 2022.

[16] Jiangbo Shi, Chen Li, Tieliang Gong, Yefeng Zheng, and Huazhu Fu. Vila-mil: Dual-scale vision-language multiple instance learning for whole slide image classification. In *Proceedings of the IEEE/CVF Conference on Computer Vision and Pattern Recognition (CVPR)*, pages 11248–11258, June 2024.

[17] Alec Radford, Jong Wook Kim, Chris Hallacy, Aditya Ramesh, Gabriel Goh, Sandhini Agarwal, Girish Sastry, Amanda Askell, Pamela Mishkin, Jack Clark, et al. Learning transferable visual models from natural language supervision. In *International conference on machine learning*, pages 8748–8763. PMLR, 2021.

[18] Maxime Oquab, Timothée Darcet, Theo Moutakanni, Huy V. Vo, Marc Szafraniec, Vasil Khalidov, Pierre Fernandez, Daniel Haziza, Francisco Massa, Alaaeldin El-Nouby, Russell Howes, Po-Yao Huang, Hu Xu, Vasu Sharma, Shang-Wen Li, Wojciech Galuba, Mike Rabbat, Mido Assran, Nicolas Ballas, Gabriel Synnaeve, Ishan Misra, Herve Jegou, Julien Mairal, Patrick Labatut, Armand Joulin, and Piotr Bojanowski. Dinov2: Learning robust visual features without supervision, 2023.

[19] Xiyue Wang, Junhan Zhao, Eliana Marostica, Wei Yuan, Jietian Jin, Jiayu Zhang, Ruijiang Li, Hongping Tang, Kanran Wang, Yu Li, Fang Wang, Yulong Peng, Junyou Zhu, Jing Zhang, Christopher R. Jackson, Jun Zhang, Deborah Dillon, Nancy U. Lin, Lynette Sholl, Thomas Denize, David Meredith, Keith L. Ligon, Sabina Signoretti, Shuji Ogino, Jeffrey A. Golden, MacLean P. Nasrallah, Xiao Han, Sen Yang, and Kun-Hsing Yu. A pathology foundation model for cancer diagnosis and prognosis prediction. *Nature*, 634(8035):970–978, Oct 2024.

[20] Julio Silva-Rodriguez, Hadi Chakor, Riadh Kobbi, Jose Dolz, and Ismail Ben Ayed. A foundation language-image model of the retina (flair): Encoding expert knowledge in text supervision. *Medical Image Analysis*, 99:103357, 2025.

[21] Kaiming He, Xiangyu Zhang, Shaoqing Ren, and Jian Sun. Deep residual learning for image recognition. In *Proceedings of the IEEE conference on computer vision and pattern recognition*, pages 770–778, 2016.

[22] Ruiqi Wu, Chenran Zhang, Jianle Zhang, Yi Zhou, Tao Zhou, and Huazhu Fu. Mm-retinal: Knowledge-enhanced foundational pretraining with fundus image-text expertise. In *International Conference on Medical Image Computing and Computer-Assisted Intervention*, pages 722–732. Springer, 2024.

[23] Zihan Li, Diping Song, Zefeng Yang, Deming Wang, Fei Li, Xiulan Zhang, Paul E Kinahan, and Yu Qiao. Visionunite: A vision-language foundation model for ophthalmology enhanced with clinical knowledge. *IEEE Transactions on Pattern Analysis and Machine Intelligence*, 2025.

[24] Yuxin Fang, Quan Sun, Xinggang Wang, Tiejun Huang, Xinlong Wang, and Yue Cao. Eva-02: A visual representation for neon genesis. *Image and Vision Computing*, page 105171, 2024.

[25] Qinkai Yu, Jianyang Xie, Anh Nguyen, He Zhao, Jiong Zhang, Huazhu Fu, Yitian Zhao, Yalin Zheng, and Yanda Meng. Clip-dr: Textual knowledge-guided diabetic retinopathy grading with ranking-aware prompting. In *International Conference on Medical Image Computing and Computer-Assisted Intervention*, pages 667–677. Springer, 2024.

[26] Chanwoo Kim, Soham U. Gadgil, Alex J. DeGrave, Jesutofunmi A. Omiye, Zhuo Ran Cai, Roxana Daneshjou, and Su-In Lee. Transparent medical image ai via an image-text foundation model grounded in medical literature. *Nature Medicine*, 30(4):1154–1165, 2024.

[27] Siyuan Yan, Xieji Li, Ming Hu, Yiwen Jiang, Zhen Yu, and Zongyuan Ge. MAKE: Multi-Aspect Knowledge-Enhanced Vision-Language Pretraining for Zero-shot Dermatological Assessment . In *proceedings of Medical Image Computing and Computer Assisted Intervention – MICCAI 2025*, volume LNCS 15964. Springer Nature Switzerland, September 2025.

[28] Siyuan Yan, Zhen Yu, Clare Primiero, Cristina Vico-Alonso, Zhonghua Wang, Litao Yang, Philipp Tschandl, Ming Hu, Lie Ju, Gin Tan, et al. A multimodal vision foundation model for clinical dermatology. *Nature Medicine*, pages 1–12, 2025.

[29] Chunyuan Li, Cliff Wong, Sheng Zhang, Naoto Usuyama, Haotian Liu, Jianwei Yang, Tristan Naumann, Hoifung Poon, and Jianfeng Gao. Llava-med: Training a large language-and-vision assistant for biomedicine in one day. In *Advances in Neural Information Processing Systems*, 2023.

[30] Yunfei Xie, Ce Zhou, Lang Gao, Juncheng Wu, Xianhang Li, Hong-Yu Zhou, Sheng Liu, Lei Xing, James Zou, Cihang Xie, and Yuyin Zhou. Medtrinity-25m: A large-scale multimodal dataset with multigranular annotations for medicine, 2024.

[31] Haotian Liu, Chunyuan Li, Qingyang Wu, and Yong Jae Lee. Visual instruction tuning. In *Advances in Neural Information Processing Systems*, 2023.

[32] Haotian Liu, Chunyuan Li, Yuheng Li, and Yong Jae Lee. Improved baselines with visual instruction tuning. In *Proceedings of the IEEE/CVF Conference on Computer Vision and Pattern Recognition (CVPR)*, pages 26296–26306, June 2024.

[33] Weiquan Huang, Aoqi Wu, Yifan Yang, Xufang Luo, Yuqing Yang, Liang Hu, Qi Dai, Xiyang Dai, Dongdong Chen, Chong Luo, and Lili Qiu. Llm2clip: Powerful language model unlock richer visual representation, 2024.

[34] Sartaj Bhuvaji, Ankita Kadam, Prajakta Bhumkar, Sameer Dedge, and Swati Kanchan. Brain tumor classification (mri), 2020.

[35] Eduardo Soares, Plamen Angelov, Sarah Biaso, Michele Higa Froes, and Daniel Kanda Abe. Sars-cov-2 ct-scan dataset: A large dataset of real patients ct scans for sars-cov-2 identification. *MedRxiv*, pages 2020–04, 2020.

[36] Jiancheng Yang, Rui Shi, and Bingbing Ni. Medmnist classification decathlon: A lightweight automl benchmark for medical image analysis. In *IEEE 18th International Symposium on Biomedical Imaging (ISBI)*, pages 191–195, 2021.

[37] Jiancheng Yang, Rui Shi, Donglai Wei, Zequan Liu, Lin Zhao, Bilian Ke, Hanspeter Pfister, and Bingbing Ni. Medmnist v2-a large-scale lightweight benchmark for 2d and 3d biomedical image classification. *Scientific Data*, 10(1):41, 2023.

[38] Daniel S. Kermany, Michael Goldbaum, Wenjia Cai, Carolina C.S. Valentim, Huiying Liang, Sally L. Baxter, Alex McKeown, Ge Yang, Xiaokang Wu, Fangbing Yan, Justin Dong, Made K. Prasadha, Jacqueline Pei, Magdalene Y.L. Ting, Jie Zhu, Christina Li, Sierra Hewett, Jason Dong, Ian Ziyar, Alexander Shi, Runze Zhang, Lianghong Zheng, Rui Hou, William Shi, Xin Fu, Yaou Duan, Viet A.N. Huu, Cindy Wen, Edward D. Zhang, Charlotte L. Zhang, Oulan Li, Xiaobo Wang, Michael A. Singer, Xiaodong Sun, Jie Xu, Ali Tafreshi, M. Anthony Lewis, Huimin Xia, and Kang Zhang. Identifying medical diagnoses and treatable diseases by image-based deep learning. *Cell*, 172(5):1122–1131.e9, 2018.

[39] Walid Al-Dhabayani, Mohammed Gomaa, Hussien Khaled, and Aly Fahmy. Dataset of breast ultrasound images. *Data in Brief*, 28:104863, 2020.

[40] Fabio A. Spanhol, Luiz S. Oliveira, Caroline Petitjean, and Laurent Heutte. A dataset for breast cancer histopathological image classification. *IEEE Transactions on Biomedical Engineering*, 63(7):1455–1462, 2016.

[41] De Cai, Jie Chen, Junhan Zhao, Yuan Xue, Sen Yang, Wei Yuan, Min Feng, Haiyan Weng, Shuguang Liu, Yulong Peng, Junyou Zhu, Kanran Wang, Christopher Jackson, Hongping Tang, Junzhou Huang, and Xiyue Wang. Hicervix: An extensive hierarchical dataset and benchmark for cervical cytology classification. *IEEE Transactions on Medical Imaging*, 43(12):4344–4355, 2024.

[42] Ruhan Liu, Xiangning Wang, Qiang Wu, Ling Dai, Xi Fang, Tao Yan, Jaemin Son, Shiqi Tang, Jiang Li, Zijian Gao, Adrian Galdran, J.M. Poorneshwaran, Hao Liu, Jie Wang, Yerui Chen, Prasanna Porwal, Gavin Siew Wei Tan, Xiaokang Yang, Chao Dai, Haitao Song, Mingang Chen, Huating Li, Weiping Jia, Dinggang Shen, Bin Sheng, and Ping Zhang. Deepdrid: Diabetic retinopathy—grading and image quality estimation challenge. *Patterns*, page 100512, 2022.

[43] Philipp Tschandl, Cliff Rosendahl, and Harald Kittler. The ham10000 dataset, a large collection of multi-source dermatoscopic images of common pigmented skin lesions. *Scientific data*, 5(1):1–9, 2018.

[44] Noel C. F. Codella, David Gutman, M. Emre Celebi, Brian Helba, Michael A. Marchetti, Stephen W. Dusza, Aadi Kalloo, Konstantinos Liopyris, Nabin Mishra, Harald Kittler, and Allan Halpern. Skin lesion analysis toward melanoma detection: A challenge at the 2017 international symposium on biomedical imaging (isbi), hosted by the international skin imaging collaboration (isic). In *2018 IEEE 15th International Symposium on Biomedical Imaging (ISBI 2018)*, pages 168–172, 2018.

[45] Carlos Hernández-Pérez, Marc Combalia, Sebastian Podlipnik, Noel CF Codella, Veronica Rotemberg, Allan C Halpern, Ofer Reiter, Cristina Carrera, Alicia Barreiro, Brian Helba, et al. Bcn20000: Dermoscopic lesions in the wild. *Scientific Data*, 11(1):641, 2024.

[46] Jingyi Zhang, Jiaxing Huang, Sheng Jin, and Shijian Lu. Vision-language models for vision tasks: A survey. *IEEE Transactions on Pattern Analysis and Machine Intelligence*, 2024.

[47] Qi Chen, Ruoshan Zhao, Sinuo Wang, Vu Minh Hieu Phan, Anton van den Hengel, Johan Verjans, Zhibin Liao, Minh-Son To, Yong Xia, Jian Chen, et al. A survey of medical vision-and-language applications and their techniques. *arXiv preprint arXiv:2411.12195*, 2024.

[48] Tristan Thrush, Ryan Jiang, Max Bartolo, Amanpreet Singh, Adina Williams, Douwe Kiela, and Candace Ross. Winoground: Probing vision and language models for visio-linguistic compositionality. In *Proceedings of the IEEE/CVF Conference on Computer Vision and Pattern Recognition (CVPR)*, pages 5238–5248, June 2022.

[49] Weijie Tu, Weijian Deng, and Tom Gedeon. A closer look at the robustness of contrastive language-image pre-training (clip). In *Advances in Neural Information Processing Systems*, 2023.

[50] Prashant Shrestha, Sanskar Amgain, Bidur Khanal, Cristian A Linte, and Binod Bhatarai. Medical vision language pretraining: A survey. *arXiv preprint arXiv:2312.06224*, 2023.

[51] Yunkun Zhang, Jin Gao, Zheling Tan, Lingfeng Zhou, Kexin Ding, Mu Zhou, Shaoting Zhang, and Dequan Wang. Data-centric foundation models in computational healthcare: A survey. *arXiv preprint arXiv:2401.02458*, 2024.

[52] Yuhao Zhang, Hang Jiang, Yasuhide Miura, Christopher D Manning, and Curtis P Langlotz. Contrastive learning of medical visual representations from paired images and text. In *Machine learning for healthcare conference*, pages 2–25. PMLR, 2022.

[53] Armand Joulin, Laurens Van Der Maaten, Allan Jabri, and Nicolas Vasilache. Learning visual features from large weakly supervised data. In *European conference on computer vision*, pages 67–84. Springer, 2016.

[54] Ting Chen, Simon Kornblith, Mohammad Norouzi, and Geoffrey Hinton. A simple framework for contrastive learning of visual representations. *arXiv preprint arXiv:2002.05709*, 2020.

[55] Ting Chen, Simon Kornblith, Kevin Swersky, Mohammad Norouzi, and Geoffrey Hinton. Big self-supervised models are strong semi-supervised learners. *arXiv preprint arXiv:2006.10029*, 2020.

[56] Yinbin Lu and Alan Wang. Integrating language into medical visual recognition and reasoning: A survey. *Medical Image Analysis*, page 103514, 2025.

[57] Julio Silva-Rodríguez, Hadi Chakor, Riadh Kobbi, Jose Dolz, and Ismail Ben Ayed. A foundation language-image model of the retina (flair): encoding expert knowledge in text supervision. *Medical Image Analysis*, 99:103357, 2025.

[58] Tianbin Li, Yanzhou Su, Wei Li, Bin Fu, Zhe Chen, Ziyan Huang, Guoan Wang, Chenglong Ma, Ying Chen, Ming Hu, et al. Gmai-vl & gmai-vl-5.5 m: A large vision-language model and a comprehensive multimodal dataset towards general medical ai. *arXiv preprint arXiv:2411.14522*, 2024.

[59] Kenneth Clark, Bruce Vendt, Kirk Smith, John Freymann, Justin Kirby, Paul Koppel, Stephen Moore, Stanley Phillips, David Maffitt, Michael Pringle, et al. The cancer imaging archive (tcia): maintaining and operating a public information repository. *Journal of digital imaging*, 26(6):1045–1057, 2013.

[60] European Organization For Nuclear Research and OpenAIRE. Zenodo, 2013.

[61] Kaggle. <https://www.kaggle.com>

[62] Jeremy Irvin, Pranav Rajpurkar, Michael Ko, Yifan Yu, Silviana Ciurea-Ilcus, Chris Chute, Henrik Marklund, Behzad Haghgoo, Robyn Ball, Katie Shpanskaya, et al. CheXpert: A large chest radiograph dataset with uncertainty labels and expert comparison. In *Proceedings of the AAAI conference on artificial intelligence*, volume 33, pages 590–597, 2019.

[63] Alistair Johnson, Tom Pollard, Roger Mark, Seth Berkowitz, and Steven Horng. Mimic-cxr database. *PhysioNet10*, 13026:C2JT1Q, 2024.

[64] Emma Dugas, Jared, Jorge, and Will Cukierski. Diabetic retinopathy detection. <https://kaggle.com/competitions/diabetic-retinopathy-detection>, 2015. Kaggle.

[65] Coen de Vente, Koenraad A. Vermeer, Nicolas Jaccard, He Wang, Hongyi Sun, Firas Khader, Daniel Truhn, Temirgali Aimyshev, Yerkebulan Zhanibekuly, Tien-Dung Le, Adrian Galdran, Miguel Ángel González Ballester, Gustavo Carneiro, R. G. Devika, Hrishikesh Panikkasseril Sethumadhavan, Densen Puthussery, Hong Liu, Zekang Yang, Satoshi Kondo, Satoshi Kasai, Edward Wang, Ashritha Durvasula, Jónathan Heras, Miguel Ángel Zapata, Teresa Araújo, Guilherme Aresta, Hrvoje Bogunović, Mustafa Arikán, Yeong Chan Lee, Hyun Bin Cho, Yoon Ho Choi, Abdul Qayyum, Imran Razzak, Bram van Ginneken, Hans G. Lemij, and Clara I. Sánchez. Airogs: Artificial intelligence for robust glaucoma screening challenge. *IEEE Transactions on Medical Imaging*, 43(1):542–557, 2024.

[66] Weixiong Lin, Ziheng Zhao, Xiaoman Zhang, Chaoyi Wu, Ya Zhang, Yanfeng Wang, and Weidi Xie. Pmc-clip: Contrastive language-image pre-training using biomedical documents. In *International Conference on Medical Image Computing and Computer-Assisted Intervention*, pages 525–536. Springer, 2023.

[67] Johannes Rückert, Louise Bloch, Raphael Brüngel, Ahmad Idrissi-Yaghbir, Henning Schäfer, Cynthia S Schmidt, Sven Koitka, Obioma Pelka, Asma Ben Abacha, Alba G. Seco de Herrera, et al. Rocov2: Radiology objects in context version 2, an updated multimodal image dataset. *Scientific Data*, 11(1):688, 2024.

[68] Sanjay Subramanian, Lucy Lu Wang, Sachin Mehta, Ben Bogin, Madeleine Van Zuylen, Sravanthi Parasa, Sameer Singh, Matt Gardner, and Hannaneh Hajishirzi. Medicat: A dataset of medical images, captions, and textual references. 2020.

[69] Negin Baghbanzadeh, Adibvafa Fallahpour, Yasaman Parhizkar, Franklin Ogidi, Shuvendu Roy, Sajad Ashkezari, Vahid Reza Khazaie, Michael Colacci, Ali Etemad, Arash Afkanpour, et al. Advancing medical representation learning through high-quality data. In *International Conference on Medical Image Computing and Computer-Assisted Intervention*, pages 24–33. Springer, 2025.

[70] Feng Liu, Miguel Hernandez-Cabronero, Victor Sanchez, Michael W Marcellin, and Ali Bilgin. The current role of image compression standards in medical imaging. *Information*, 8(4):131, 2017.

[71] David Koff, Peter Bak, André Matos, and Geoff Norman. Evaluation of irreversible compression ratios for medical images thin slice ct and update of canadian association of radiologists (car) guidelines. *Journal of digital imaging*, 26(3):440–446, 2013.

[72] HMSS Herath, HMKKMB Herath, Nuwan Madusanka, and Byeong-Il Lee. A systematic review of medical image quality assessment. *Journal of Imaging*, 11(4):100, 2025.

[73] Richard J Chen, Tong Ding, Ming Y Lu, Drew FK Williamson, Guillaume Jaume, Bowen Chen, Andrew Zhang, Daniel Shao, Andrew H Song, Muhammad Shaban, et al. Towards a general-purpose foundation model for computational pathology. *Nature Medicine*, 2024.

[74] John N Weinstein, Eric A Collisson, Gordon B Mills, Kenna R Shaw, Brad A Ozenberger, Kyle Ellrott, Ilya Shmulevich, Chris Sander, and Joshua M Stuart. The cancer genome atlas pan-cancer analysis project. *Nature genetics*, 45(10):1113–1120, 2013.

[75] Leland McInnes, John Healy, and James Melville. Umap: Uniform manifold approximation and projection for dimension reduction, 2020.

[76] Tim Sainburg, Leland McInnes, and Timothy Q Gentner. Parametric umap embeddings for representation and semisupervised learning. *Neural Computation*, 33(11):2881–2907, 2021.

[77] Lars Buitinck, Gilles Louppe, Mathieu Blondel, Fabian Pedregosa, Andreas Mueller, Olivier Grisel, Vlad Niculae, Peter Prettenhofer, Alexandre Gramfort, Jaques Grobler, Robert Layton, Jake VanderPlas, Arnaud Joly, Brian Holt, and Gaël Varoquaux. API design for machine learning software: experiences from the scikit-learn project. In *ECML PKDD Workshop: Languages for Data Mining and Machine Learning*, pages 108–122, 2013.

[78] Vitali Petsiuk, Abir Das, and Kate Saenko. Rise: Randomized input sampling for explanation of black-box models. In *Proceedings of the British Machine Vision Conference (BMVC)*, 2018.

[79] Gabriel Goh, Nick Cammarata, Chelsea Voss, Shan Carter, Michael Petrov, Ludwig Schubert, Alec Radford, and Chris Olah. Multimodal neurons in artificial neural networks. *Distill*, 6(3):e30, 2021.

[80] Karen Simonyan and Andrew Zisserman. Very deep convolutional networks for large-scale image recognition. In Yoshua Bengio and Yann LeCun, editors, *3rd International Conference on Learning Representations, ICLR 2015, San Diego, CA, USA, May 7-9, 2015, Conference Track Proceedings*, 2015.

[81] Feng Li, Renrui Zhang, Hao Zhang, Yuanhan Zhang, Bo Li, Wei Li, Zejun Ma, and Chunyuan Li. Llava-next-interleave: Tackling multi-image, video, and 3d in large multimodal models. *arXiv preprint arXiv:2407.07895*, 2024.

[82] Thomas Wolf, Lysandre Debut, Victor Sanh, Julien Chaumond, Clement Delangue, Anthony Moi, Pierrick Cistac, Tim Rault, Rémi Louf, Morgan Funtowicz, Joe Davison, Sam Shleifer, Patrick von Platen, Clara Ma, Yacine Jernite, Julien Plu, Canwen Xu, Teven Le Scao, Sylvain Gugger, Mariama Drame, Quentin Lhoest, and Alexander M. Rush. Transformers: State-of-the-art natural language processing. In *Proceedings of the 2020 Conference on Empirical Methods in Natural Language Processing: System Demonstrations*, pages 38–45, Online, October 2020. Association for Computational Linguistics.